ChemComm

Preferential CO_2 Adsorption by an Ultra-microporous Zinc-Aminotriazolato-Acetate MOF

Journal:	*ChemComm*
Manuscript ID	CC-COM-03-2023-001157.R1
Article Type:	Communication

COMMUNICATION

Preferential CO_2 Adsorption by an Ultra-microporous Zinc-Aminotriazolato-Acetate MOF

Received 00th January 20xx,
Accepted 00th January 20xx

DOI: 10.1039/x0xx00000x

Piyush Singh,[a,b] Himan Dev Singh,[a,b] Abhijith Hari Menon,[a,b] and Ramanathan Vaidhyanathan[a,b]*

ABSTRACT

Ultramicroporous MOF enables tight packing of the active functional groups, directly impacting the selective guest-framework interactions. MOFs with pores simultaneously lined by methyl and amine may serve as the ultimate humid CO_2 sorbent. However, structural complexity prevents reaching full advantage even in a simple zinc-triazolato-acetate layered-pillared MOF.

Capturing CO_2 present in different concentrations along with other gases is vital to managing global CO_2 concentrations. [1, 2] Sorbents play a key role here, and metal-organic frameworks (MOFs) form an important class of designable sorbents.[3-8] MOF functionalized with basic groups aids selective adsorption of CO_2 from gas mixtures. In this context, azolate MOFs have gained a special position due to their tridentately linking azole rings, which form stable structural motifs when combined with ions of Zn, Co, Ni, Mn, Fe etc.[9-18] They can have zeolitic structures or a layered-pillared structure, and some show excellent scalability and ability to do humid CO_2 capture.[19-28] Short pillars result in ultra-microporous MOFs, which can converge the basicity of the azolate with the molecular sieving to gain a high CO_2 selectivity.[21,22,26] While many such layered-pillared MOFs with azolates are reported,[21-31] some of the readily accessible pillaring agents have been elusive in generating the sort-out 3D ultra-microporous structures. Achieving this robust 3D framework from simple ligand combinations depends on identifying optimized reaction conditions and its selective CO_2 sorption relies on the binding group's orientations within the pore. All things considered, we particularly want to form a Zn-Atz (Atz = 3-amino-1,2,4-triazolate) layer pillared by acetate ligands. The idea being two short linkers will give rise to ultra-micropores lined by basic triazolate rings and polarizing acetate oxygens, and the CO_2-philic amine groups can decorate their walls. The methyl groups of the acetate should provide the required hydrophobic lining to keep water away, thus making the MOF suited for humid CO_2 capture. We successfully optimized the condition for isolating this Zn-Atz-Acetate MOF with a 3D structure. However, completing the 3D framework from only these ligands (Atz and acetate) required the charge-balancing from a free hydroxide anion that resides in the pore.[32,33] The sway of this simple structure with diverse chemical sites on CO_2 adsorption is discussed here.

IISERP-MOF28, Zinc aminotriazolato acetato hydroxide, $Zn_2(CH_3COO)(C_2N_4H_4)_2.(OH^-)(H_2O)_x$, **1**, was synthesized solvothermally in a DMF+water system. The role of the solvent is crucial, as using the more commonly used solvent system, water + methanol or ethanol,[21] leads to the formation of a 2D layered solid with acetate groups hanging into the interlayer spaces.[10] Using only neat DMF or water does not work. The solvent mixture employed here provides the right basic condition for the generation of hydroxide species. The building unit of **1** consists of one tetrahedrally coordinated Zn-atom connected to three different triazolate units and an acetate oxygen (Figure S1A). Every triazolate unit links three Zinc centers and propagates into a Zn-Atz layer (Figure S1B). The adjacent Zn_2Atz_2 dimeric units in this layer are rotated by ~ 90° with respect to each other, hence lie on two perpendicular planes (Figure S1). This generates a buckled ZnAtz layer, which enables the adjacent layers stacked along the b-axis to come closer enough to be pillared by the acetate oxygen (μ-2 bridging acetates) into a 3D framework (Figure 1A). Note that the acetates are half-occupied for a fully occupied Zn and aminotriazolate unit, necessitating the hydroxide to participate as a charge-balancing counter anion. The hydroxides reside between the carboxylate units of the acetate; thus, they form a row of anionic charges along the pore walls. Acetate oxygnes, hydroxide ions and the triazole rings line the channels running along the a-axis

[a] Department of Chemistry, Indian Institute of Science Education and Research, Dr. Homi Bhabha Road, Pashan, Pune 411008, India.
[b] Centre for Energy Science, Indian Institute of Science Education and Research, Dr. Homi Bhabha Road, Pashan, Pune 411008, India.
Electronic Supplementary Information (ESI) available: [details of any supplementary information available should be included here]. See DOI: 10.1039/x0xx00000x

(7.9 x 6.6 Å, not factoring the van der Waal radii, Figure 1A). Unfortunately, the spaces decorated by the free-amine and the methyl groups do not form solvent-accessible channels (Figure 1B and 1C).

The powder XRD confirmed the bulk purity of the MOF (Figure S2). The MOF is stable till 260 °C, and the triazolate and carboxylate functionalities are amply incorporated (Figure S3 and S4). A smooth type 1 adsorption isotherm marks its permanent porosity for N_2 at 77 K (Figures 2 and S5). We applied the Rouquerol consistency criteria to determine the sample's Brunauer-Emmett-Teller (BET) area.[34] A fit to the adsorption branch yielded a BET area of 497 m^2/g (Figure S5). Nonlocalized Density Functional Theory (NLDFT) fit amounts the pore diameter to be ~5 Å (Figure 2A), which agrees well with the single crystal structure. **1** demonstrated good adsorption properties, with a maximum CO_2 absorption of 3.1 mmol/g at 1 bar and 298 K (Figure 2B) and a saturation CO_2 capacity of 4.0 mmol/g (195 K CO_2 isotherm). At 0.15 bar and 25 °C, **1** adsorbs 2.2 mmol/g CO_2, representing the CO_2's partial pressure of a typical post-combustion flue gas. Notably, **1** exhibited less N_2 uptake at room temperature (Figure S6). This high performance from such a simple structured and formulated MOF is noteworthy. The Ideal Adsorbed Solution Theory (IAST) calculation performed using the isotherms collected at 298 and 313 K, employing a nominal composition of $15CO_2$:$85N_2$, yields a CO_2/N_2 selectivity of 75 and 150, respectively (Figures 2C and S8). Although the selectivity values are not as high as those of the recently reported UMMOFs,[35-39] these are sufficient to achieve the benchmarked 99% purity during separation.[Refs-40] The calculated HOA using both virial and DFT models at 313, 298, and 273 K CO_2 isotherms was 34 kJ/mol at zero loading (Figures 2D and S7) and reaches 27–28 kJ/mol at higher loadings. The moderate heat suggests facile regeneration of **1** after use.

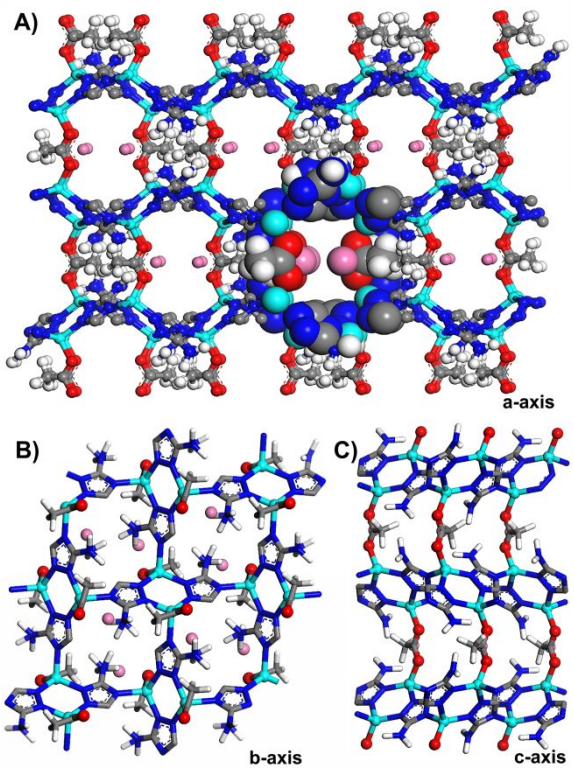

Figure 1. A) Three-dimensional structure of IISERP-MOF28 showing the channels along the a-axis lined by acetate oxygens and occupied by hydroxide ions shown in pink. . B) and C) represent the view along the b- and c-axes having spaces decorated by amine and the methyl groups, unfortunately too narrow for guest access.

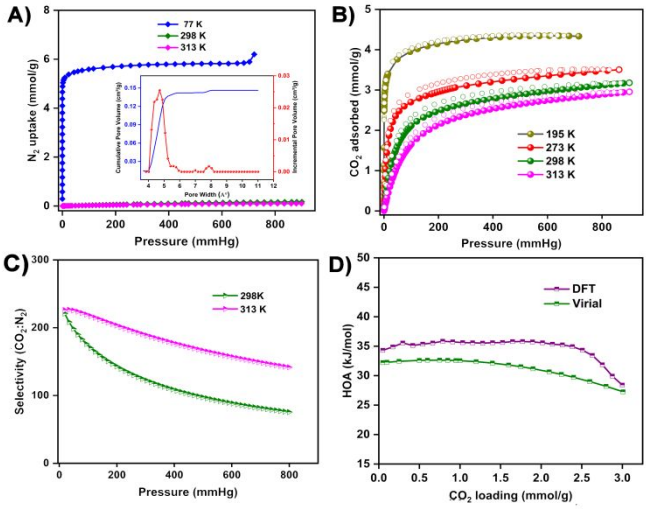

Figure 2. (A) N_2 sorption isotherm and (B) CO_2 sorption isotherms of **1** at different temperatures. Inset: the pore size distribution. (C) CO_2/N_2 selectivity calculated using IAST model employing a nominal composition of $15CO_2$: $85N_2$. (D) The HOA plots from the virial and DFT modelling done using the CO_2 isotherms at 273, 283, and 298 K.

Any MOF's critical requirements in its possible industrial applications are crystallinity and porosity retention, and cost-effective scalability. Some MOFs have better-reported properties in one or more of the abovementioned criteria, but only a few meet all the requirements.[21,41] We checked the chemical stability of **1**; maintained it at different pH conditions by soaking in HCl (acidic) and KOH (basic). The MOF showed no structural changes even after 15 days, as validated by their powder XRDs (Figure 3A) The MOF was stable to soaking in water for 20 days (Figure S9) and exhibited no structural changes. Some recent physisorptive CO_2 capture processes follow a steam-assisted regeneration[21] which mandates steam stability on the candidate MOFs. We exposed **1** to controlled humidity conditions (RH=25% to RH=99%) at a constant temperature (25 °C), and the PXRD patterns indicated a negligible loss of crystallinity (Figures 3 and S10). Also, its crystallinity survived when we heated it from 25° to 75°C at 99% RH (Figure 3B). The intrinsic hydrolytic stability of the MOF is further supported by a water vapor isotherm and a post-adsorption PXRD (Figures 3C). The water vapour isotherm also indicates that though the MOF powder is hydrophobic (Figure S10), intrinsically **1** is hydrophilic. Further, the 298K CO_2 uptakes of the post-chemically treated samples confirmed the retention of its permanent porosity (Figure 3E). Additionally, the cyclic studies demonstrate that even after 10 cycles, the CO_2 uptake essentially remains the same (Figure 3F). These tests are meaningful in establishing that even monodentate pillaring acetate units combined with the triazolate can afford one of the simplest compositions carrying more than sufficient

stability for humid CO_2 capture. Also, **1** could be scaled to multi grams using the solvothermal methods (Figures S11).

Different CO_2 interaction sites in IISERP-MOF28 (triazolate ring, amine groups, hydroxide ions and acetate oxygens), compelled us to investigate the CO_2 locations within the pore (Figure 4A). For this purpose, we simulated the 273K CO_2 adsorption isotherms using GCMC methods embedded in the Accelrys program. The simulated isotherm matched well with the experimental one (Figure 4B). We obtained the optimized CO_2 positions from the lowest energy configuration established using a simulated annealing routine (See SI for details). The final structure optimized to an average energy of -65 kcal/mole/UC (Figure 4A), wherein the CO_2's were located proximal to the hydroxide ions and the acetate oxygens at acceptable distances.[42,43] The oxygens of the CO_2 and the framework's functional groups were oriented for hydrogen-bond type interactions (Figure 4A). The simulations yield an average HOA of 32 kJ/mol, which agrees well with the experimental value. Meanwhile, an RDF analysis confirmed the presence of CO_2…OH^- (O…O separation = ~2.7 Å) and CO_2…acetate (O…O separation = ~2.9 Å) interactions (Figure 4C). Notably, no CO_2 was found proximal to the amine moiety owing to the lack of space (Figure 4C).

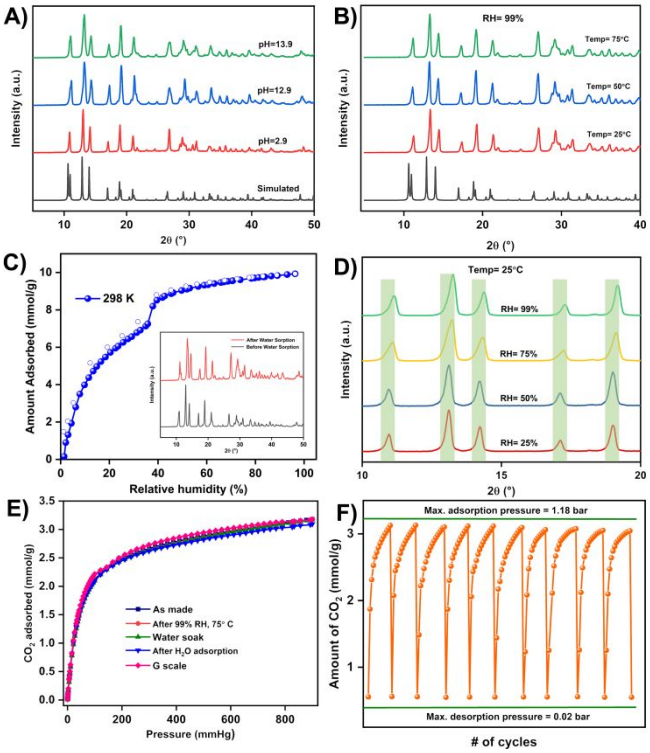

Figure 3. PXRDs of **1** kept at (A) different pH condition. (B) different temperatures and constant relative humidity. (C) The water adsorption isotherm of **1** at 298K. Inset: the PXRD of the post adsorption phase. (D) PXRDs of **1** kept at different relative humidity and constant temperature (E) Comparative CO_2 adsorption isotherms of **1**: after soaking in water for one month (blue); after water adsorption (sky blue); gram scale synthesis (pink). (F) iso-cycling for 1: 10 cycles of a pressure swing of 1.2–0.02 bar.

Several zinc-triazolate frameworks have been reported in the literature over the last twenty years.[10-12,16,17,20,28-31,44] One of the main attractions of these systems has been their readily available ligand and zinc being a benign and relatively cheaper metal. Also, the amphoteric and borderline hard-soft acid-base nature of the Zn^{2+} allows it to bind strongly with N-rich triazole and carboxylate ligands. This accounts for the high chemical stability in this family of azolate MOFs. Among the 3D layered-pillared azolate-carboxylate MOFs, those with short pillars are ultra-microporous and exhibit preferential CO_2 uptake characteristics.[21-24,26] Few others have Zinc azolate layers decorated with dangling carboxylate moieties (formate, acetate)[10,29,30,31] or 3D pillaring carbonate or formate.[12] The $ZnAtzCO_3$ is closely related to the present MOF with an identical structure, except that **1** includes the free charge-balancing hydroxide ions in the channels. This makes this acetate MOF chemically more robust than the carbonate analogue.

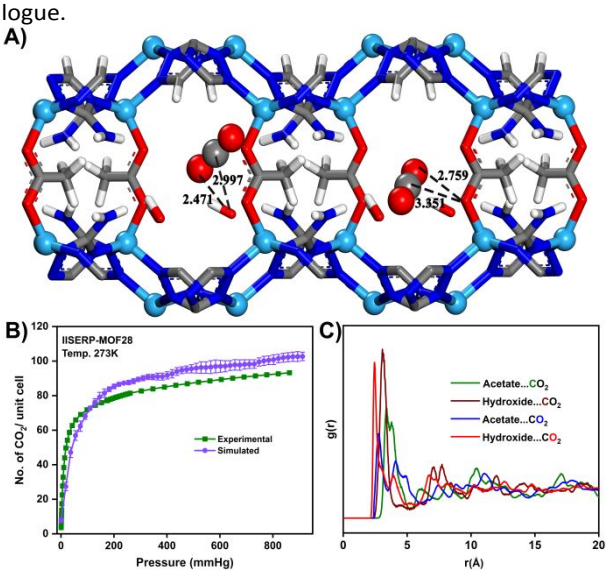

Figure 4. (A) and (B) Structure of CO_2@**1** obtained from the GCMC modelling and the associated simulated isotherm are shown. The most favourable interaction distances are mentioned. (C) RDF plots from the MD simulations showing the averaged interaction distances for CO_2 with various sites of the framework.

Encouraged by the promise of triazolate MOFs in humid CO_2 capture[21-23,28] we investigated the metal-ligand binding strength of these structures using computational methods. Binding energy gives an idea about stability. For this, we simulated 3 x 3 x 3 cells of different Zinc azolate MOFs and calculated their binding energy using the DMOL^3. In all cases, we employed solvent-free frameworks to ensure the estimates were entirely metal-ligand related. For **1**, the hydroxide was retained in the pores. The comparison is presented in Figure S12. The 3D layered-pillared ZnAtzOx[22,23] and the 3D zeolitic framework, MAF-7,[44] had the highest binding energy. Surprisingly, the relative binding energy of CALF-20 (3D ZnTzOx)[21] was low. One major difference in CALF-20 compared to all other frameworks is the lack of pendent amino or methyl groups, which takes away a substantial amount of electrostatic and van der Waal interactions. Also, another 3D ZnAtzOxalate, reported by Aparna et al., with dynamic swiveling oxalate pillars (monodentate),[24] had only half the binding energy of the other 3D ZnAtzOx (bidentate oxalates).[22] While framework stability is one aspect, it is worth realizing that the 3D network of the CALF20 ($P2_1/c$) though topologically comparable to the ZnAtzOx (Pbca),[22] has

more ordered triazolates and less ordered oxalate, while the latter has it reversed. This gives more openness to the CALF-20. Thus, the presence of pendant/templating amino or methyl group though it helps improve the overall binding strength, leaves the structure less open. Hence improving the binding energy of the CALF-20 lattice or increasing the openness of the other amino-triazolate MOFs could yield superior sorbents for humid CO_2 capture.

In summary, a 3D cationic framework zinc-aminotriazolato-acetate with guest hydroxide ions in their ultra-micropores is formed. It has most of the attributes required for a humid CO_2 capture and shows good selective uptake of CO_2 with excellent cyclic stability. Disappointingly, the amine groups (CO_2-philic) and the methyl groups (water-repelling) do not line the gas-accessible pores even in this uncomplicated layered (ZnAtz)-pillared(acetate) structure. Consequently, this 3D framework with the simplest composition is yet to bring out these ligands' full potential for humid CO_2 capture. A structural comparison of zinc-azolate MOFs reveals that azolates have the potential to provide high binding energies and open-framework structure. The optimal condition to access both these features in the same structure could hold the key; the pursuit is on.

Conflicts of interest

"There are no conflicts to declare".

Notes and references

1 D. W. Keith, *Science*, 2009, **325**, 1654–1655.
2 Z. Sun, Y. Liao, S. Zhao, X. Zhang, Q. Liua and X. Shi, *J. Mater. Chem. A*, 2022,**10**, 5174-5211.
3 D. M. D'Alessandro, B. Smit and J. R. Long, *Angew. Chem. Int. Ed.*, 2010, **49**, 6058–6082.
4 M. Oschatz and M. Antonietti, *Energy Environ. Sci.*, 2018, **11**, 57–70.
5 Q. Zhai, Q. Lin, T. Wu, L. Wang, S. Zheng, X. Bu and P. Feng, *Chem. Mater.*, 2012, **24**, 2624.
6 Z. Zhang, Z.-Z. Yao, S. Xiang and B. Chen, *Energy Environ. Sci.*, 2014, **7**, 2868–2899.
7 S. Mukherjee, N. Kumar, A. A. Bezrukov, K. Tan, T. Pham, K. A. Forrest, K. A. Oyekan, O. T. Qazvini, D. G. Madden, B. Space and M. J. Zaworotko, *Angew. Chem., Int. Ed.*, 2021, **60**, 10902–10909.
8 R.-B. Lin, S. Xiang, W. Zhou and B. Chen, *Chem.*, 2020, **6**, 337–363.
9 Z. S. Wang, M. Li, Y. L. Peng, Z. Zhang, W. Chen and X. C. Huang, *Angew. Chem. Int. Ed.*, 2019, **58**, 16071–16076.
10 A. Zhu, J. Lin, J. Zhang and X. Chen, *Inorg. Chem.*, 2009, **48**, 3882.
11 R. Lin, D. Chen, Y. Lin, J. Zhang and X. Chen, *Inorg. Chem.*, 2012, **51**, 9950.
12 Y. Lin, Y. Zhang, J. Zhang and and X. Chen, *Cryst. Growth Des.*, 2008, **8**, 3673.
13 X.-L. Hu, F.-H. Liu, H.-N. Wang, C. Qin, C.-Y. Sun, Z.-M. Su and F.-C. Liu, *J. Mater. Chem. A*, 2014, **2**, 14827.
14 S. Chand, G. Verma, A. Pal, S. C. Pal, S. Q. Ma and M. C. Das, *Chem. – Eur. J.*, 2021, **27**, 11804–11810.
15 X. Zhao, X. Bu, E. T. Nguyen, Q.-G. Zhai, C. Mao and P. Feng, *J. Am. Chem. Soc.*, 2016, **138**, 15102–15105.
16 J. P. Zhang, Y. B. Zhang, J. B. Lin and X. M. Chen, *Chem. Rev.*, 2012, **112**, 1001–1033.
17 Q. Zhai, N. Bai, S. Li, X. Bu and P. Feng, *Inorg. Chem.*, 2015, **54**, 9862.
18 J.-N. Lu, J. Liu, L.-Z. Dong, S.-L. Li, Y.-H. Kan and Y.-Q. Lan, *Chem. – Eur. J.*, 2019, **25**, 15830–15836.
19 B. Wang, A. P. Coˆte´, H. Furukawa, M. O'Keeffe and O. M. Yaghi, *Nature*, 2008, **453**, 207–211.
20 C. Y. Su, A. M. Goforth, M. D. Smith, P. J. Pellechia and H. C. zurLoye, *J. Am. Chem. Soc.*, 2004, **126**, 3576–3586.
21 J.-B. Lin, T. T. T. Nguyen, R. Vaidhyanathan, J. Burner, J. M. Taylor, H. Durekova, F. Akhtar, R. K. Mah, O. Ghaffari-Nik, S. Marx, N. Fylstra, S. S. Iremonger, K. W. Dawson, P. Sarkar, P Hovington, A. Rajendran, T. K. Woo and G. K. H. Shimizu, *Science*, 2021, **374**, 1464.
22 R. Vaidhyanathan, S. S. Iremonger, K. W. Dawson, G. K. Shimizu, *Chem. Commun.*, 2009, **35**, 5230–5232.
23 R. Vaidhyanathan, S. S. Iremonger, G. K. H. Shimizu, P. G. Boyd, S. Alavi and T. K. Woo, *Science*, 2010, **330**, 650.
24 A. Banerjee, S. Nandi, P. Nasa and R. Vaidhyanathan, *Chem. Commun.,* 2016, **52**, 1851-54.
25 R. Vaidhyanathan, S. S. Iremonger, G. K. H. Shimizu, P. G. Boyd, S. Alavi and T. K. Woo, *Angew. Chem., Int. Ed.*, 2012, **51**, 1826–1829.
26 R. Vaidhyanathan, I. Martens, J. Lin, S. S. Iremonger and G. K. H. Shimizu, *Can. J. Chem.*, 2016, **94**, 449.
27 X.-D. Fang, L.-B. Yang, A.-N. Dou, A.-X. Zhu, Q.-Q. Xu, *J. Struct. Chem.*, 2018, **59**, 1450–1455.
28 Z. Shi, Y. Tao, J. Wu, C. Zhang, H. He, L. Long, Y. Lee, T. Li and Y.-B. Zhang, *J. Am. Chem. Soc.*, 2020, **142**, 2750–2754.
29 Z. L. Chen, X. L. Li and F. P. Liang, *J. Solid State Chem.*, 2008, **181**, 2078.
30 J. Liu, L. Y. Yang and F. Luo, *J. Solid State Chem.*, 2021, **301**, 122369.
31 B. Liu and X. C. Zhang, *Inorg. Chem. Commun.*, 2008, **11**, 1162.
32 P. Liao, H. Chen, D. Zhou, S. Liu, C. He, Z. Rui, H. Ji, J. Zhang and X. M. Chen, *Energy Environ. Sci.*, 2015, **8**, 1011.
33 S. Yang, J. Sun, A. J. Ramirez-Cuesta, S. K. Callear, W. I. F. David, D. P. Anderson, R. Newby, A. J. Blake, J. E. Parker, C. C. Tang and M. Schröder, Nat. Chem., 2012, **4,** 887–894.
34 J. Rouquerol , P. Llewellyn and F. Rouquerol , *Stud. Surf. Sci. Catal.*, 2007, **160**, 49.
35 K. Adil, Y. Belmabkhout, R. S. Pillai, A. Cadiau, P. M. Bhatt, A. H. Assen, G. Maurin and M. Eddaoudi, *Chem. Soc. Rev.*, 2017, **46**, 3402–3430.
36 P. M. Bhatt, Y. Belmabkhout, A. Cadiau, K. Adil, O. Shekhah, A. Shkurenko, L. J. Barbour and M. Eddaoudi, *J. Am. Chem. Soc.*, 2016, **138**, 9301–9307.
37 S. Shalini, S. Nandi, A. Justin, R. Maity and R. Vaidhyanathan, *Chem. Commun.*, 2018, **54**, 13472–13490.
38 S. Mukherjee, N. Sikdar, D. O'Nolan, D. M. Franz, V. Gasco´n, A. Kumar, N. Kumar, H. S. Scott, D. G. Madden, P. E. Kruger, B. Space and M. J. Zaworotko, *Sci. Adv.*, 2019, **5**, 1–8.
39 S. Nandi, S. Collins, D. Chakraborty, D. Banerjee, P. K. Thallapally, T. K. Woo, R. Vaidhyanathan, *J. Am. Chem. Soc.*, 2017, **139**, 1734–1737.
40 S. G. Subraveti, S. Roussanaly, R. Anantharaman, L. Riboldi, A. Rajendran, *Sep. Purif. Technol.* 2021, **256**, 117832.
41 H. A. Evans, D. Mullangi, Z. Deng, Y. Wang, S. B. Peh, F. Wei, J. Wang, C. M. Brown, D. Zhao, P. Canepa and A. K. Cheetham, *Sci. Adv.*, 2022, **8**, eade1473.
42 S. Nandi, P. D. Luna, T. D. Daff, J. Rother, M. Liu, W. Buchanan, A. I. Hawari, T. K. Woo and R. Vaidhyanathan, *Sci. Adv.*, 2015, **1**, e1500421.
43 S. Nandi, H. D. Singh, D. Chakraborty, R. Maity, R.Vaidhyanathan, *Appl. Mater. Interfaces*, 2021, **13**, 24976–24983.
44 J.-P. Zhang, A.-X. Zhu, R.-B. Lin, X.-L. Qi and X.-M. Chen, *Adv. Mater.*, 2011, **23**, 1268.

